Simulation and Analysis of ACDR-oriented Vertebral Endplate Cutting Process

Heqiang Tian[1*], Peng Yang[1], Jun Zhao[2], Chunjian Su[1]

[1]*Mechanical and Electronic Engineering College*
Shandong University of Science and Technology
Qingdao 266590, China
E-mails: thq_1980@126.com, 514294993@qq.com, suchunjian2008@163.com

[2]*State Key Laboratory of Robotics and System*
Harbin Institute of Technology,
Harbin 150080, China
E-mail: 601012783@qq.com

[*]*Corresponding author*

Abstract: *In the artificial cervical disc replacement (ACDR), the polishing quality of fitting surface between vertebral endplate and artificial intervertebral disc has a direct relation with operation result. For this reason, an in-depth study is necessary on the vertebral endplate cutting process. This paper is intended to simulate and analyze the cutting process of vertebral endplate using numerical computation method. Firstly, a plane cutting model is established through an analysis on the cutting process to simulate the single-edge cutting process, and the temperature distribution calculation is carried out using the mean heat flux of continuous cutting. Secondly, a vertebral endplate material constitutive model is established on the basis of the endplate anatomy and mechanical property, so that some problems are analyzed about simulation algorithm, frictional contact and chip separation in the vertebral endplate cutting finite element (FE) simulation. Finally, stress distribution, cutting force, endplate deformation and residual stress and cutting temperature, as well as simulation results, are analyzed in vertebral endplate cutting process. The FE simulation may simplify vertebral endplate cutting, improve analytical precision, avoid plenty of repetitive cutting experiments, and reduce research cost greatly. Moreover, it gives full and fine description to the whole continuous, dynamic cutting process. All of this lay solid theoretical basis for an in-depth study of influence of different cutting parameters on endplate cutting as well as improvement of operation effect.*

Keywords: *Vertebral endplate, Cutting model, Finite element simulation, Cutting force, Cutting temperature.*

Introduction

The vertebral endplate is the connecting part of vertebral body and intervertebral disc, located on the upper and lower curved surface of the vertebral body, and made up of cartilage and bone endplates, its good mechanical performance can prevent vertebral body from deforming and damaging, which has important significance for maintaining and protecting the normal geometry of vertebral body. As shown in Fig. 1, in artificial cervical disc replacement surgery, artificial cervical disc prosthesis is implanted to simulate activity of normal cervical disc and achieve function of buffer shocks after anterior decompression and removal of cervical disc by using the grinding equipment (Fig. 2), which has become an effective and primary mean used for the cervical disease treatment. The most important feature for the study on vertebral endplate cutting is that the cut material should be bioactive bone tissue, and this study is different from other ones on endplate cutting. It is a non-homogenous,

viscoelastic bio-composite material with anisotropy. The endplates are different in thickness in different segments of vertebra, and are different even if it is at the same segment in different positions. It is seen from the previous research results that the characteristics of all parts of the endplate are obviously different due to different structure, density and mineral contents.
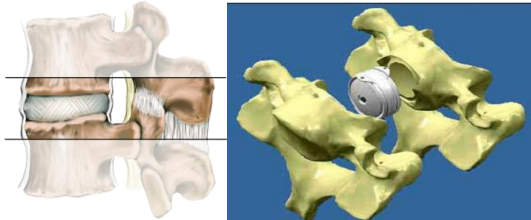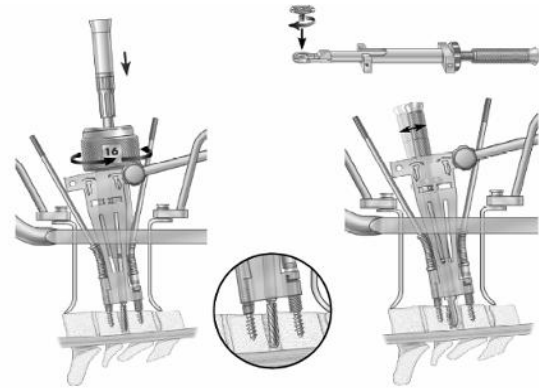
Fig. 1 Artificial cervical disc replacement

Fig. 2 Grinding equipment for artificial cervical disc replacement surgery

In the artificial cervical disc replacement (ACDR), the abrasive drilling is mainly used to polish the fitting surface between vertebral endplate and artificial intervertebral disc at vertebral lesion. The ideal polished endplate surface should be fitted with implantation materials, where, the dotted force should be avoided to reduce post-operational settlement of fusion cage, and bony union is available in the end. In addition, the method and position of vertebral endplate excision and the imbedding position of implantation materials have a greater influence on post-operational sedimentation rate of fusion cage. Polishing quality of the fitting surface between vertebral endplate and artificial intervertebral disc has a direct relation with operation effect and stability, effectiveness and lifetime of imbedded intervertebral disc. For this reason, an in-depth study is necessary on the cutting process of vertebral endplate. The cutting analysis is a complicated process by the analytical way, where many problems are handled approximately at a bigger deviation. Accurate value can be got with enormous experimental workload and higher cost, but the exterior cutting process and essence are not understood clearly yet. It simplifies the cutting problem with higher analytical accuracy using the numerical computation method to analyze the vertebral endplate cutting process. By this way, plenty of repetitive cutting experiments can be avoided, and research cost is reduced greatly. Moreover, the continuous, dynamic cutting process can be showed in a short time, and the whole cutting process can be described in details. On the basis of that, the influence of different cutting parameters on endplate cutting effect can studied deeply. This is of major practical significance for improvement of operation effect and efficiency. For this reason, this paper is intended to conduct the numerical simulation of the vertebral endplate cutting. First, a vertebral endplate cutting model is established. Second, contact analysis and chip separation are studied for such key problems as simulation calculation. Finally, analyses are done on stress distribution, cutting fore, endplate deformation, residual stress and cutting temperature in vertebral endplate cutting.

Research status
The vertebral endplate bone tissue cutting is a highly non-linear heating coupling process, where, a part of work done by cutting force turns into heat. Castillo et al. [2] measured the changes that occur in bone matrix as a consequence of the increased temperature and establishing categories of histological morphology in relation to fire temperature.

The research on cutting is involved in materials science, material cutting theory, heat transfer theory, cutting temperature measurement, numerical solution and simulation. Cutting material by cutter can be seen as the movement of heat source on cutting face at a feed speed, that is to say, moving heat source in the material machining process [5]. Rosenthal [12] and Jaeger [6] had made relatively outstanding contribution to the study of the moving heat source, which laid solid foundation for theoretical research of cutting. Afterwards, some modified model was set forth on the basis of Jaeger model. Ehrhard et al. [3] believed that the plane heat source was made up of numerous point heat sources, and got the approximate solution about the question. The temperature distribution in the bone tissue interior can be obtained by the approximate solution. Loewen and Shaw [10] put forth an average temperature theoretical calculation method for the contacting area of shearing surface and rake face. As a theoretical way to calculate cutting temperature, it provides a basis for calculating the distribution ratio of cutting heat in chip, cutter and workpiece.

The development of numerical computation method and progress of computer technology make it possible to analyze cutting force and temperature field quickly by numerical method. There are two approaches to analyze the heat transfer described by heat conduction equation, boundary conditions and initial conditions, that is, FE method and finite difference method. Sugita et al. [15] and Shin and Yoon [14] conducted theoretical computation and experimental verification for the cutting temperature of bone interior in orthopedic surgery using linear heat source moving on the semi-infinite plane, and predicted cutting temperature distribution. Hong and Lo [4] established a linear reverse heat transfer model to predict cutting temperature distribution and heat flux along the cutting direction. Kim et al. [8] applied continuous reverse heat conduction algorithm to determine cutting temperature. Brosse et al. [1] studied the heat flux coming into workpiece in cutting process using reverse heat transfer method and temperature measurement method based on thermal infrared imager. Zhang et al. [17] built a heat transfer model and an FE model, and predicted the bone grinding temperature of skull base neurosurgery using reverse heat transfer method by modeling and simulation. Tai et al. [16] explored the feasibility of using motor electrical feedback to estimate temperature rise during a surgical bone grinding procedure, where PWM can be used as feedback for heat generation and temperature prediction. Grey based fuzzy algorithm [11] is used to optimize multiple performance characteristics in drilling of bone. Sezek et al. [13] analyzed the temperature changes during cortical bone drilling for different parameters such as drill rotation speed, feed-rate, drill diameter, drill force, bone mineral density and bone sex via the finite element method, FEM. Karaca et al. [7] investigated the temperature changes at the drill site throughout the statistical and histopathological analysis by considering the bone mineral density, bone sex, drill tip angle, drill speed, drill force and feed-rate. Lee et al. [9] presented a parametric study on the effects of machining conditions and drill-bit geometries on the resulting temperature field in the bone and the drill bit by a new thermal model with applications to orthopaedic surgery.

Establishment of vertebral endplate cutting model
Establishment of cutting force model
The cutting slip deformation only occurs on the surface perpendicular to the cutter edge without regard to workpiece deformation in the milling cutter axis, and the stress and strain for each plane perpendicular to the cutting edge should be consistent. Thus, the vertical milling may be seen as a 2D plane strain problem. The plane orthogonal cutting model is a most basic and also a most classical analytical model in the cutting process, where a lot of complex cutting modes can be simplified as an orthogonal cutting model for study and analysis. For each cutting edge, the cutting thickness for the edge changes with the cutter

rotating and the mutual movement of cutter and vertebral endplate. In climb milling, the cutter rotates in the same direction of feed, and the cutting changes from thin to thick. In up milling, the cutter rotates in the opposite to the direction of feed, and the cutting changes from thick to thin. If the each edge cutting process is simplified as the equal-thickness cutting model, it will be in a discrepancy with the actual situation. Aiming at this feature of milling, this paper will further correct the plane orthogonal cutting model as a thickening plane cutting model so as to simulate the single edge cutting in the milling process, as shown in Fig. 3.
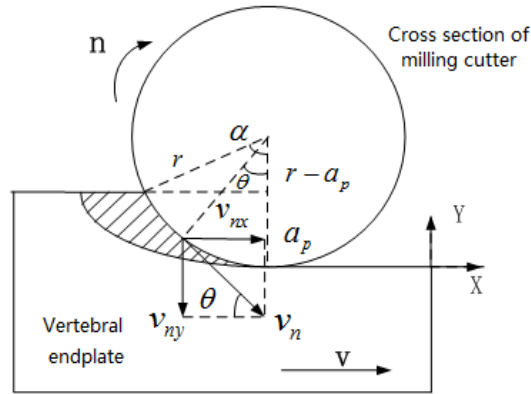

Fig. 3 Schematic diagram of plane milling

The turned angle for each tooth in the milling process:

$$\partial = \arccos \frac{r - a_p}{r} \tag{1}$$

The time for each tooth in the milling process:

$$t = \frac{60}{2\pi n} \arccos \frac{r - a_p}{r} \tag{2}$$

Rotating linear speed for milling cutter:

$$\upsilon_n = \frac{2\pi rn}{60} \tag{3}$$

Angle between radius of cutter and the finished plane normal at the time t:

$$\theta = \frac{2\pi nt}{60} \tag{4}$$

Translational distance of milling cutter during milling for each tooth:

$$\partial_f = \upsilon T \tag{5}$$

Kinematic speed of tool nose at the time t includes the rotating circular speed and average straight-line rate:

$$V = \sqrt{\upsilon_n^2 + 2\upsilon\upsilon_n \cos \frac{2\pi nt}{60} + \upsilon^2} \tag{6}$$

Total contact length of cutting edge and the cut workpiece during milling for each tooth:

$$L = \int_0^T \sqrt{\upsilon_n^2 + 2\upsilon\upsilon_n \cos\frac{2\pi nt}{60} + \upsilon^2} \, dt \tag{7}$$

where α and T are respectively the turn angle of milling cutter during cutter for each tooth (°) and time (s); a_p − thickness for milling (m); r − outer diameter of milling cutter (m); n − rotate speed of milling cutter; υ − translational speed of milling cutter.

The simplified model by plane orthogonal cutting in endplate milling is gotten as shown in Fig. 4. L stands for total contact length of milling cutter single edge and vertebral endplate in cutting each time; a_p is the cutting thickness for each time. The follow-up endplate cutting FE analysis is done according to the model by the plane orthogonal cutting.
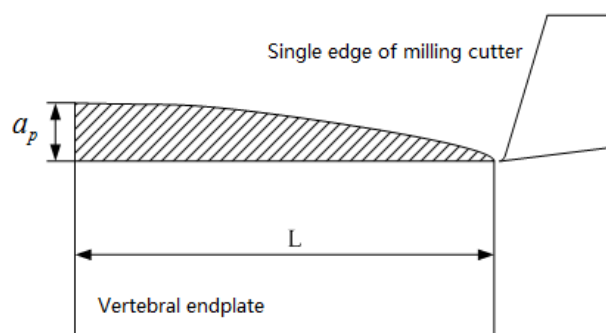

Fig. 4 Schematic diagram of plane thickening cutting

Establishment of cutting thermal model

It is seen from Fig. 1 that when the medical flat-end shank cutter is used to cut vertebral endplate, a curved surface is produced by cutting the vertebral endplate by the cutter at a high rotating speed, and the cutting heat is transferred from the surface heat source to vertebral endplate. Thus, the heat produced in the interrupted cutting of vertebral endplate by milling cutter edge can be simulated by the periodic heating of curved surface heat source to the vertebral endplate. At this moment, the temperature rises in a periodic fluctuation way in the endplate interior. Actually, the temperature fluctuation from periodic cutting only exerts an impact on contacting position of the finished workpiece and cutter at a quite small range, and the temperature becomes stable in a small distance away from the contacting position. In order to improve calculating speed and shorten calculating time, the continuous cutting is applied to simplify the non-continuous cutting in the endplate cutting. The average heat flux density is taken in a cutting period of each cutter edge. As a result, the heat is equal from the cutting heat source to workpiece at a time within cutting time. There is a small difference of temperature distribution worked out by continuous and interrupted cutting methods, but the calculating speed is improved greatly. In this paper, the temperature distribution calculation is done by average heat flux density of continuous cutting.

The cutting heat in the cutting process mainly comes from the shear slip deformation in the first cutting deformation area as well as the friction between the cutter rake face and bone in the second cutting deformation area. The contacting friction mainly affects the temperature of cutter rake face and cutting chips. What this paper focuses on is the cutting heat mainly from shear slip surface affecting bone temperature, that is, this paper will ignore the friction heat in the second deformation area. The workpiece is machined in feed movement continually. At some moment, the heat flux density distributes in a triangular way for the cut curved

surface heat source, and there is a maximum normal heat flux density at the middle of arc surface. As shown in Fig. 5, OC is the direction of maximum heat flux density.
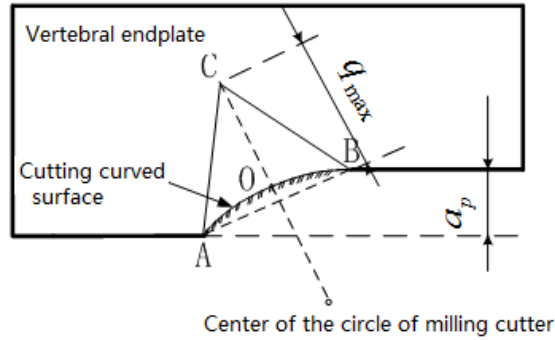

Fig. 5 Distribution of milling heat flux density in vertebral endplate

There is a quite less convection of bone and air as well as bone radiation, both of which may be ignored herein. In order to calculate temperature distribution of vertebra in cutting, it is first to calculate the maximum heat flux density transmitted to cervical Vertebra, that is, the heat flux density in the OC direction. The maximum heat flux density is expressed by Eq. (8) for milling with a flat-end shank cutter:

$$q_{max} = \frac{2F_{sh}\upsilon_{sh}R}{Jba_p\csc\varphi} \tag{8}$$

where a_p is the cutting thickness (m); $b-$ cutting depth (m); $J-$ heat equivalent of work; $F_{sh}-$ shear force on the shearing surface (N); $\upsilon_{sh}-$ shear speed (m/s); $\varphi-$ shear angle (°); in high-speed cutting, $\varphi = (90+\gamma_0)/2$, γ_0 is front rake angle; $R-$ specific value of generated heat transmitted to workpiece, as shown in Eq. (9):

$$R = 1 - \frac{1}{1+1.33\sqrt{\dfrac{\omega r_{sh}}{v_c a_p}}} \tag{9}$$

where r_{sh} is the shear strain, $r_{sh} = \cot\varphi + \tan(\varphi - \gamma_0)$; v_c- cutting speed (m/s); $K-$ heat conductivity (W/(m·°C)); $\omega-$ thermal diffusivity (m/h), $\omega = k/(c\rho)$, $c-$ workpiece specific heat (J/(kg·°C)); $\rho-$ density of workpiece (kg/m).

The maximum heat flux density transmitted to workpiece in high-speed milling by substituting Eq. (9) into Eq. (8).

The heat flux Φ produced in milling with milling cutter and transferred to bone within unit time is expressed by Eq. (10)

$$\Phi = 0.5q_{max}ba_p \tag{10}$$

When the element division is carried out for bone body using FE analysis software, the mesh must be generated accurately at the heating position of moving heat source, while the contact position away from cutter and bone cutting may be rough. The actual milling axial dimension of bone is far greater than the milling width. So, the end face effect can be ignored in its axial

direction, which is simplified as the plane strain for solution in question. This is a transient thermal analysis. It needs to set heat source position, moving mode and speed as well as the node along track direction; heat a time step in every node, then move to the next node for heating; take the previous thermal analysis result as the initial condition of new thermal analysis. So repeat this process again and again. The thermal conduction of bone should meet the Eq. (11):

$$\lambda \left(\frac{\partial^2 T}{\partial x^2} + \frac{\partial^2 T}{\partial y^2} + \frac{\partial^2 T}{\partial z^2} \right) - \rho c \upsilon_c \frac{\partial T}{\partial x} = \rho c \frac{\partial T}{\partial t} \tag{11}$$

where T is the temperature at any point on the bone (°C); υ_c − cutting speed (m/s); λ− heat conductivity (W/(m·°C)); c − specific heat capacity (J/(kg·°C)); P − bone density (kg/m^3); t − time (s).

The boundary condition should meet the following expressions:

$$\begin{cases} T = T_\infty \\ -\lambda \dfrac{\partial T}{\partial t} \\ -\lambda \left(\dfrac{\partial T}{\partial x} + \dfrac{\partial T}{\partial y} + \dfrac{\partial T}{\partial z} \right) = 2q_{max} \dfrac{x}{L} \\ T(x, y, z, 0) = T_0 \end{cases} \tag{12}$$

where T is the temperature (°C) at any point of semi-infinite body surface; q_{max} − maximum heat flux distributed in the triangular way (W); T_0 − initial temperature (°C); L − length (m) of heat source along x direction.

Based on above method, calculate and analyze the distance boundary $a_p/2$ point, that is, temperature changes in actual cutting position.

Establishment of the vertebral endplate cutting FE model
Vertebral endplate constitutive model
A macroscopic constitutive model is established aiming at the macroscopic property of vertebral endplate in consideration of complexity of actual vertebral endplate anatomy. Supposing the vertebral endplate is macro-isotropous, the transient high-temperature softening is taken no account of in cutting vertebral endplate at a high speed. The Johnson-Cook model is a constitutive model describing thermoviscoplastic deformation behavior of materials in a large deformation, high temperature and high strain rate. Moreover, it covers the influence of three factors (hardening property, stain hardening property and temperature softening effect) on material flow stress. Supposing the material is an isotropic one, it should be applied in the cutting transient simulation analysis. The flow stress expression is as follows:

$$\sigma_y = \left(A + B \bar{\varepsilon}^{p^n} \right) \left(1 + c \ln \varepsilon^* \right) \left(1 - T^{*m} \right) \tag{13}$$

where $\bar{\varepsilon}^p$ is the effective plastic strain; ε^* − standard effective plastic strain rate (1/s); A − yield strength (MPa); B − work hardening modulus (MPa); n − hardening coefficient;

c − strain rate constant; m − thermal softening constant. A, B, n, c and m all are material constants.

Parameters of endplate Johnson-Cook model are presented in Table 1.

Table 1. Parameters of endplate Johnson-Cook model

A, (MPa)	B, (MPa)	n	c	m
218	546	0.355	3.73	0.038

The first and second items in Eq. (13) are corresponding to material strain rate sensitivity and temperature sensitivity effects respectively. The relation of shearing modulus of elasticity with Poisson's ratio and Young's modulus of elasticity is:

$$G = \frac{E}{2(1+\nu)} \tag{14}$$

Physical characteristic parameters of cutter are presented in Table 2.

Table 2. Physical characteristic parameters of cutter

Material density, (g/cm^3)	Elasticity modulus, (MPa)	Poisson's ratio
3.55	850	0.08

The relation of material pressure and volume defined by Gruneisen state equation is realized by two different ways. The pressure of compressing material defined by Gruneisen equation with the 3D striking velocity-particle speed is as follows:

$$p = \frac{\rho_0 C^2 \mu \left[1 + \left(1 - \frac{\gamma_0}{2}\right)\mu - \frac{a}{2}\mu^2 \right]}{\left[1 - (S_1 - 1)\mu - S_2 \frac{\mu^2}{\mu+1} - S_3 \frac{\mu^3}{(\mu+1)^2} \right]^2} + (\gamma_0 + a\mu) E \tag{15}$$

For expanding material:

$$p = \rho_0 C^{2\mu} + (\gamma_0 + a^\mu) E \tag{16}$$

where S_1, S_2 and S_3 are the $vs-vp$ curve slope coefficient; C − $vs-vp$ curve intercept; γ_0 − Gruneisen gamma parameter; a − first-order volume correction value of γ_0 and $\mu = \rho / \rho_0 - 1$.

Simulation algorithm
The main principle of Lagrange algorithm is that FE mesh is adhered to material and deforms with deformation and flow of material. However, if the analyzed structure deforms greatly, the FE mesh will distort severely due to deformation of material, internal numerical calculation is carried out hardly, and the procedure operation terminates in the end. The features for Euler algorithm are: the FE mesh is fixed, and the material flows in meshes.

By this way, the mesh distortion can be cancelled. Thus, the Euler algorithm is more applicable to simulate the deformation of controllable fluid of volume. The ALE algorithm selects Lagrange and Euler algorithms by switching over based on model real-time situations. It can give full play to their advantages, solve numerical calculation caused by severe distortion of FE, and realize dynamic analysis of fluid-structure interaction. In this paper, the ALE algorithm is selected as cutting simulation algorithm.

Definition of contact friction

These complex contact frictions may have important influences on cutting. The existing contact algorithm can be divided into three classes: single face contact, point-face contact and face-face contact. Ten specific contact algorithms are available for each contact algorithm. The single face contact is the most common one. This is because the contact area is not defined at all for single contact, and the penetration for the procedure judgment is realized on the external surface of automatic search model. This most fits for real-time change large deformation occurrence of contact area for cutting simulation. Thus, the 2D single face automatic contact type is selected in this paper to represent contact friction between cutter and endplate.

Generation of FE meshes

The material can be broken and removed in the cutting process, and its cutting deformation area unit deforms greatly, which is involved in its damage and failure. Thus, it is important to set reasonable unit mesh division for convergence of cutting FE simulation calculation, and this directly concerns the final results are reasonable or not. The ANSYS/LS-DYNA software can provide rich unit types. Plane162 is the explicit dynamic plane unit in 4 nodes and 6 degrees of freedom with sand control. In this paper, the cutting model is supposed as a plane model, so the Plane162 is selected as a basic unit to establish the cutting FE model.

Selection of chip separation criteria

The principle for geometric separation criteria are used to judge whether the chip separation occurs or not based on the FE unit nodes of the workpiece machined at the cutter nose and the nose nearby. With the chip layer set as an independent part artificially, three contact pairs are available to define mutual friction contact relation between cutting, cut workpiece and cutter, as shown in Fig. 6. The contact pair (I) is to represent the interaction between cut material and chip. Its chip node is bond with the machined workpiece node at the initial moment; when the element stress at a distance before the cutter nose reaches the predefined separation threshold, the node at this position can be separated into the finished workpiece node and chip node automatically to form chips. The interrelation of extrusion, friction and heat transfer between the rake face of cutter and chip can be simulated by the contact pair (II). The contact pair (III) represents the interaction of friction and extrusion between the finished surface of cut material and the flank surface of cutter. Compared with physical separation criteria, the geometric separation criteria have such advantages as fast calculation speed and simple definition, but such disadvantages as non-physical significance and lower accuracy.

The physical separation criteria are defined by the physical quantity of element node in the front cutter nose. The element nodes are separated when the set physical quantity value is greater than the given physical condition in any element. The common physical separation criteria include stress criterion, equivalent plastic strain criterion, and strain energy density criterion. The application of physical separation criteria means the FE simulation studied in cutting is closer to the practical situation. Thus, the effective strain of the material applied for the chip separation criteria in this paper is regarded as a reference physical index.
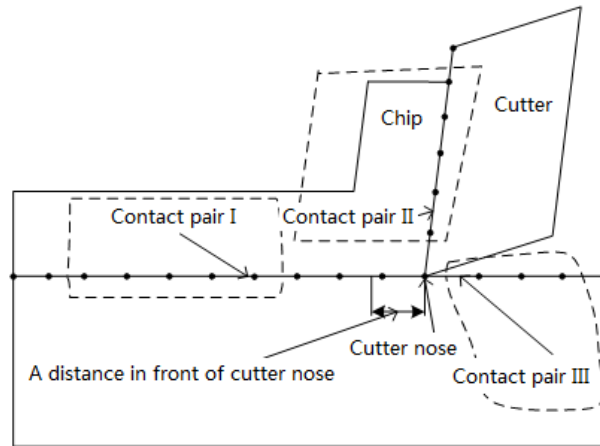
Fig. 6 Geometric separation criteria of 2D cutting FE model

The effective strain in Johnson-Cook model can be expressed by Eq. (17):

$$\varepsilon_f = \left[d_1 + d_2 \exp\left(d_3 \frac{\sigma_p}{\sigma_e} \right) \right] \left[1 + d_4 \ln\left(\frac{\dot{\varepsilon}^p}{\dot{\varepsilon}_0} \right) \right] \times \left[1 + d_5 \left(\frac{T - T_r}{T_m - T_r} \right) \right] \tag{17}$$

where $\left(\dot{\varepsilon}^p / \dot{\varepsilon}_0 \right)$ is the speed ratio of material plastic strain (s^{-1}); d_1, d_5 − separation parameter; ε_f − strain in breakage of material; σ_e − Von Mises stress (MPa); σ_p − mean stress of primary stress (MPa).

When the element strain ε_f value of cut material meets the $\varepsilon_f = 1$ of chip separation criteria, this element is separated from the cut material, and is turned into the chip.

FE simulation and analysis in vertebral endplate cutting process

For the analysis on cutting process, cutting force and temperature as well as their change rules are main research contents. The stress and strain distribution in endplate cutting process and cutting force and temperature in applying different cutting parameters can be studied based on the established endplate cutting FE analysis model. According to characteristics of artificial cervical disc replacement (ACDR), the following hypotheses should be made in the simulation of plane orthogonal cutting:

(1) Vertebral endplate is an easily-cutting material without regard to wear and tear;

(2) Vertebral endplate is regarded as an isotropous homogeneous material approximately;

(3) Cutter is seen as a rigid body, and vertebral endplate is regarded as an elastic plastic body as the hardness of cutter is far more than that of workpiece. The deformation of cutter is taken no account of in cutting simulation process.

In ANSYS/LS-DYNA, the cutter is applied with cutting speed and thickness, and the displacement is confined in *y* and *z* direction of vertebral endplate model. The cutter is fed along the +*x* direction, and the end face of endplate model is fixed by full degree of freedom. The parameters of FE simulation in the cutting process see Table 3.

Table 3. Technological parameters of vertebral endplate cutting simulation

Radius of blunt circle for cutting edge, (µm)	Cutting speed, (m/s)	Cutting thickness, (mm)	Angle of cutting edge, (°)	Angle of backing-off of cutting edge, (°)
5	1	1	18	15

Analysis on stress in cutting area

Fig. 7 a)-d) show that contact and crash of cutter and vertebral endplate, cutting, chips forming and stress distribution of FE simulation in a stable cutting condition in the orthogonal cutting of vertebral endplate. It is seen from Fig. 7 that in the cutter feeding process, the greater stress and strain form first at the contact position of vertebral endplate and cutter nose, then the stress and strain spread further along contacting face and shear angle with the cutter advancing, forming the first cutting deformation area and the second cutting deformation area. Repeatedly, the vertebral endplate chips come into being in the end. From the stress distribution at the cutting deformation area, it is found that the first shear slip deformation area in the stable cutting is a main stress-centralizing position in the vertebral cutting; the bigger stress is also applied to the frictional contact with the cutter rake face and the position nearby of cutter nose.
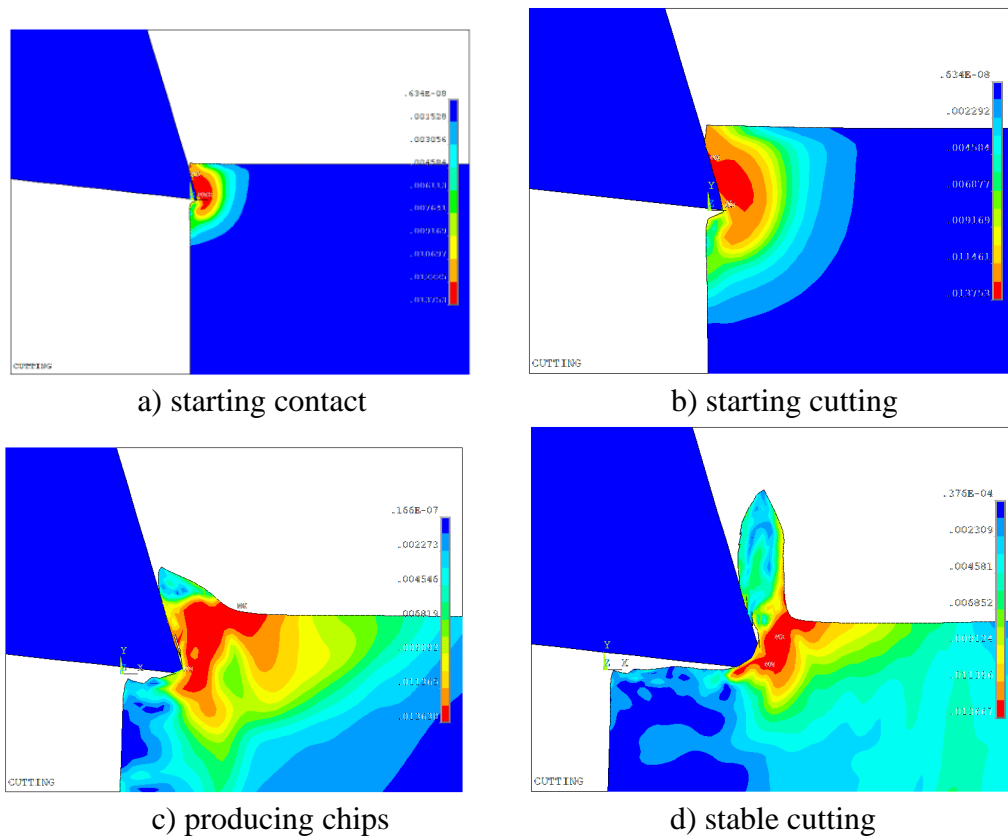

a) starting contact

b) starting cutting

c) producing chips

d) stable cutting

Fig. 7 Cloud picture of endplate cutting stress distribution

Analysis of cutting force

As the cutter is defined as a rigid body, no deformation of the rigid body is considered in the FE calculation, and the cutting force value can't be obtained from cutter FE model. The node is fixed by boundary constraint of vertebral endplate, and the specific actual cutting force value is represented by the stress change in the cutting direction. The stress change value of each node is derived from ANSYS postprocessor, and the resultant force value is obtained

with programming and summation by MATLAB, as shown in Fig. 8. Fig. 8 a)-c) show the force in *x*, *y* directions and the resultant force in the *x-y* plane respectively. It is known from the figure that the force and resultant force for the cutter in *x*, *y* directions are zero in the cutting process all the time. The cutting force value becomes bigger after the cutter contacts workpiece, and then it rises and falls at a certain value.
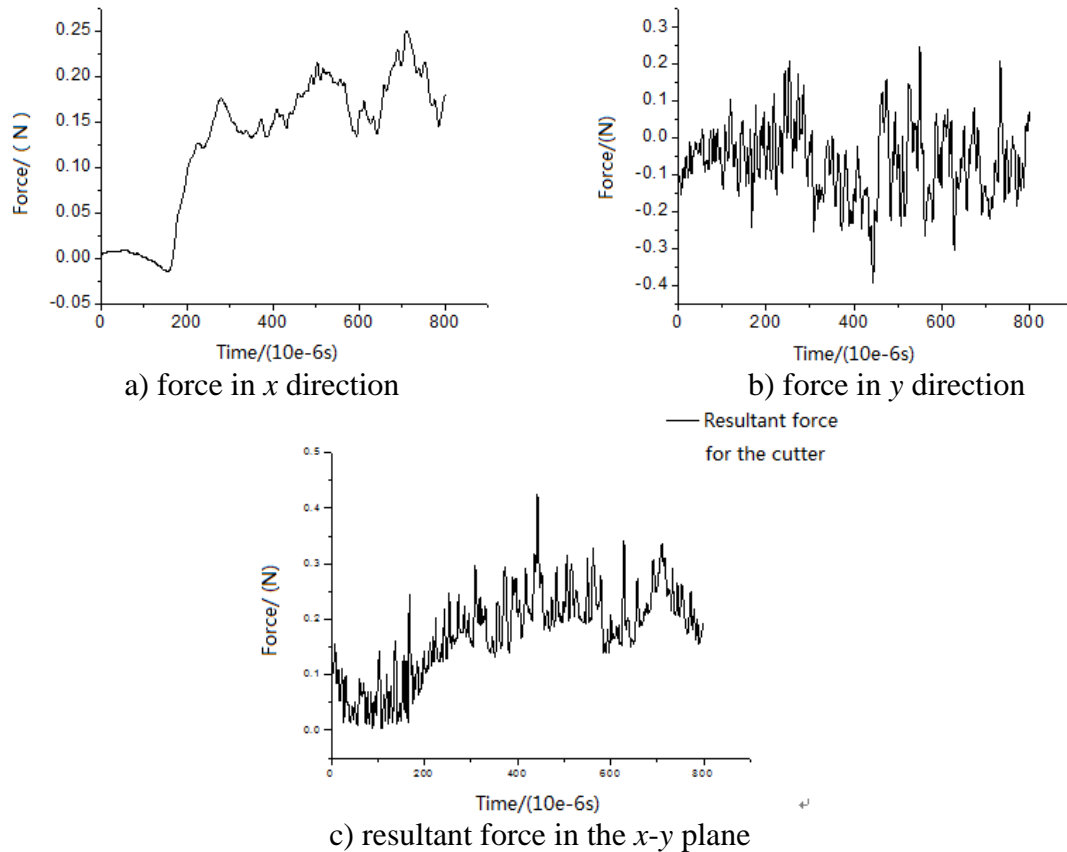
a) force in *x* direction

b) force in *y* direction

c) resultant force in the *x-y* plane

Fig. 8 Cutting force in the plane orthogonal cutting

The cutting force value for each step length is filtered and averaged after the cutting stabilizing, so as to obtain the approximate cutting force value in the stable cutting. Fig. 9 gives the changing of cutting force with cutting speed. It is seen from the figure that the cutting force reduces with the increase of cutting speed. This is because the shear angle becomes big while the shear surface becomes small in the cutting deformation area with cutting speed. On the other hand, increasing cutting speed also results in the local temperature going up within cutting area. This change can cause a less plastic flow stress which reduces the cutting force within cutting area.

Analysis on plastic strain and residual stress

As shown in Fig. 10, residual stress and plastic strain exist on the finished surface, the deformation changes greatly in the endplate cutting, and around 1mm of displacement occurs on the finished surface in the *x* direction. The plastic strain is bigger after cutting with a surface roughness ranging from several micrometers to few tens of micrometers. In the simulation results, all residual stresses existing in the finished surface are pressure stress at around 2 MPa, and its thickness ranges from around dozens to hundreds of micrometers. The residual stress and plastic strain values are bigger near the finished surface, but become less and less away from the surface. The maximum residual stress value is taken on the finished surface to study the relation of residual stress and cutting speed. It is shown in

Fig. 11 that the residual stress reduces with cutting speed, which is of no significance. This is because with rising of cutting speed, the cutting force goes down and plastic strain of vertebral endplate becomes less. However, due to the specific viscoelastic characteristics of endplate as the biological tissue, it may release stress slowly after cutting, so that the residual stress on the surface is not too bigger.
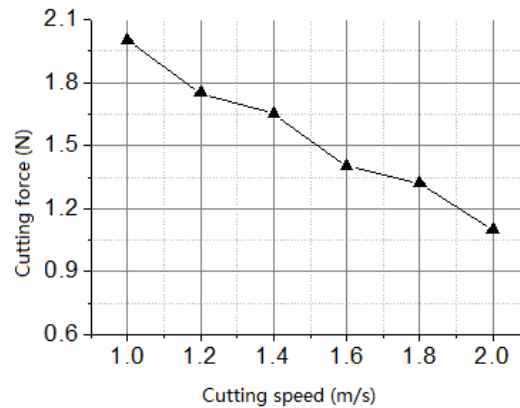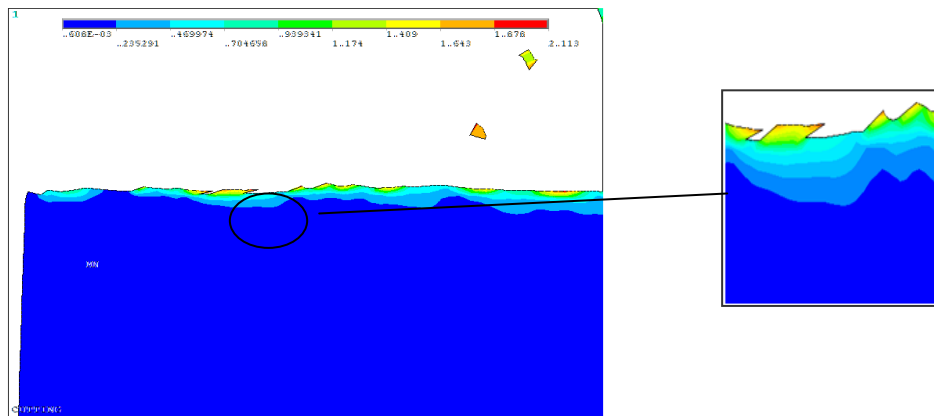

Fig. 9 Relation of cutting force and speed

Fig. 10 Features and residual stress on the finished surface

Analysis on cutting temperature
The FE simulation is done for cutting temperature by the cutting force values gained from simulation. Fig. 12 shows the cloud picture of temperature distribution inside of workpiece when the cutter cuts one position of the bone, as well as the changes of temperature with time at the point 0.5 mm away from the hot spot. It is seen that with point heat source shifting to feature point, the workpiece temperature rises up to maximum temperature significantly, then goes down slowly. When cutting speed is changed, the relation of maximum temperature and cutting speed is shown in Fig. 13. Obviously, its maximum temperature goes up slowly with cutting speed but at a gradual rate. The rising of maximum temperature is possibly because the heat produced in cutting has no time to transfer to chips with cutting speed; more and more heat stops in machined materials so that its temperature goes up. The slow rising of maximum temperature should be related to the increase of speed of chip producing. Production and outflow of a great deal of chips may slow down the rising speed of temperature.
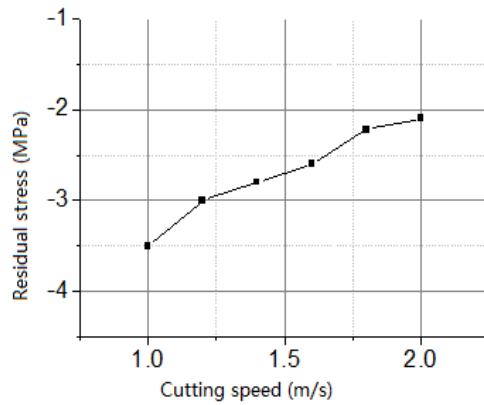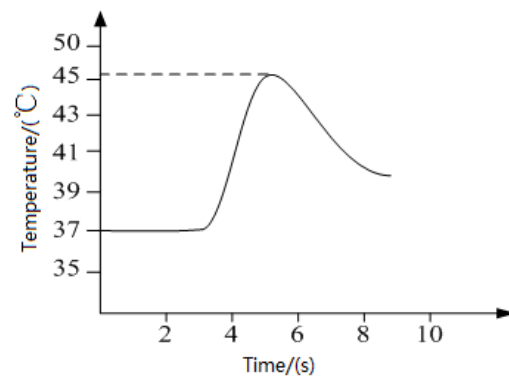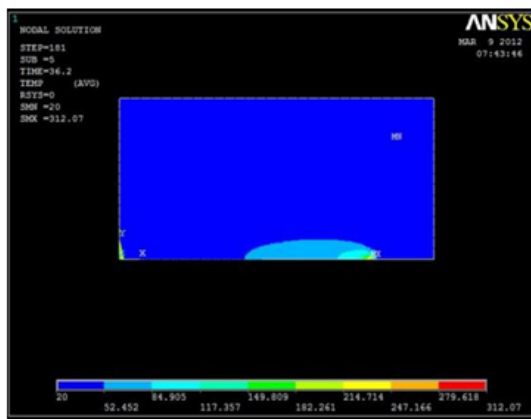
Fig. 11 Change of residual stress with cutting speed

a) cloud picture of temperature distribution   b) change of temperature with time

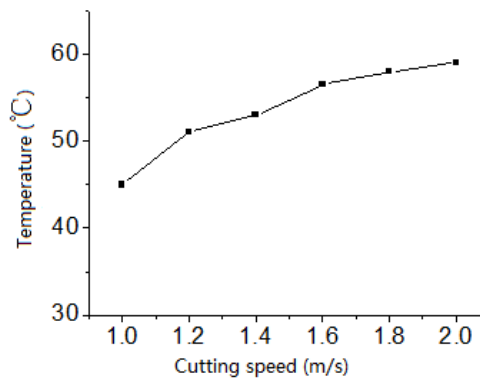Fig. 12 Distribution of 2D cutting temperature field

Fig. 13 Change of cutting temperature with cutting speed

Conclusions

This paper mainly deals with realization and analysis of number simulation for vertebral endplate cutting of the artificial cervical disc replacement (ACDR). Firstly, it analyzes the cutting process of vertebral endplate, modifies the plane orthogonal cutting model into a thickening plane cutting model to simulate the situation in single cutting process, and carries out calculation of temperature distribution using the continuous cutting mean heat flux method. Then, the vertebral endplate material constitutive model is established on the basis of endplate anatomy and mechanical characteristics. Such problems as simulation algorithm, friction contact and chip separation in vertebral endplate cutting FE simulation are analyzed. Finally, it analyzes stress distribution, cutting force, endplate deformation, residual stress and

cutting temperature in the vertebral endplate cutting, as well as the available simulation results. All of this lay the solid theoretical foundation for the in-depth study of the influence of different cutting parameters on endplate cutting as well as improvement of operation effect.

Acknowledgements

References
1. Brosse A., P. Naisson, H. Hamdi, J. M. Bergheau (2008). Temperature Measurement and Heat Flux Characterization in Grinding Using Thermography, Journal of Materials Processing Technology, 201(1-3), 590-595.
2. Castillo R. F., D. H. Ubelaker (2012). Effects of Temperature on Bone Tissue. Histological Study of the Changes in the Bone Matrix, Forensic Science International, 226, 33-37.
3. Ehrhard P., C. Holle, C. Karcher (1993). Temperature and Penetration Depth Prediction for a Three-dimensional Field below a Moving Heat Source, International Journal of Heat and Mass Transfer, 36, 3997-4008.
4. Hong K. K., C. Y. Lo (2000). An Inverse Analysis for the Heat Conduction during a Grinding Process, Journal of Materials Processing Technology, 105(1), 87-94.
5. Hou Z. B., R. Komanduri (2000). General Solutions for Stationary/moving Plane Heat Source Problems in Manufacturing and Tribology, International Journal of Heat and Mass Transfer, 43(10), 1679-1698.
6. Jaeger J. C. (1942). Moving Sources of Heat and the Temperature of Sliding Contacts, J Proc Roy Soc, New South Wales, 76, 203-224.
7. Karaca F., B. Aksakal, M. Kom (2011). Influence of Orthopaedic Drilling Parameters on Temperature and Histopathology of Bovine Tibia: An *in vitro* Study, Med Eng Phys, 33(10), 1221-1227.
8. Kim H. J., N. K. Kim, J. S. Kwak (2006). Heat Flux Distribution Model by Sequential Algorithm of Inverse Heat Transfer for Determining Workpiece Temperature in Creep Feed Grinding, Int J of Machine Tools and Manufacture, 46(15), 2086-2093.
9. Lee J. E., Y. Rabin, O. B. Ozdoganlar (2011). A New Thermal Model for Bone Drilling with Applications to Orthopaedic Surgery, Med Eng Phys, 33(10), 1234-1244.
10. Loewen E. G., M. C. Shaw (1954). On the Analysis of Cutting Tool Temperatures, Trans ASME, 76(2), 217-231.
11. Pandey R. K., S. S. Panda (2014). Optimization of Bone Drilling Parameters Using Grey-based Fuzzy Algorithm, Measurement, 47(1), 386-392.
12. Rosenthal D. (1946). The Theory of Moving Sources of Heat and Its Application to Metal Treatments, ASME, 849, 11-68.
13. Sezek S., B. Aksakal, F. Karaca (2012). Influence of Drill Parameters on Bone Temperature and Necrosis: A FEM Modeling and *in vitro* Experiments, Computational Materials Science, 60(3), 13-18.
14. Shin H. C., Y. S. Yoon (2006). Bone Temperature Estimation during Orthopaedic Round bur Milling Operations, Journal of Biomechanics, 39(1), 33-39.

15. Sugita N., T. Osa, M. Mitsuishi (2009). Analysis and Estimation of Cutting-temperature Distribution during End Milling in Relation to Orthopedic Surgery, Med Eng Phys, 31(1), 101-107.
16. Tai B. L., L. Zhang, A. Wang, S. Sullivanb, A. J. Shih (2013). Neurosurgical Bone Grinding Temperature Monitoring, Procedia CIRP, 5, 226-230.
17. Zhang L., B. L. Tai, G. Wang, K. Zhang, S. Sullivan, A. J. Shih (2013). Thermal Model to Investigate the Temperature in Bone Grinding for Skull Base Neurosurgery, Med Eng Phys, 35(10), 1391-1398.

Heqiang Tian, Ph.D.
E-mail: thq_1980@126.com

Heqiang Tian received his Ph.D. degree in Mechanical Electronic Engineering from Harbin Institute of Technology, China, in 2011. Since 2012, he has been a lecturer of Mechanical and Electronic Engineering College, Shandong University of Science and Technology, China. His research interests include biomedical engineering and medical robotics.

Peng Yang, B.Sc.
E-mail: 514294993@qq.com

Peng Yang received his B.Sc. degree in Mechanical Design and Manufacturing and Automation from Qingdao Technological University. Now he is a postgraduate at Mechanical and Electronic Engineering College, Shandong University of Science and Technology, China. His current research interests include process simulation and numerical analysis.

Jun Zhao, B.Sc.
E-mail: 601012783@qq.com

Jun Zhao received his B.Sc. degree in Mechanical Electronic Engineering from Harbin Institute of Technology. His current research interest includes biomedical engineering.

Assoc. Prof. Chunjian Su, Ph.D.
E-mail: suchunjian2008@163.com

Chunjian Su received his Ph.D. degree in Material Forming and Control Engineering from Yanshan University, China, in 2007. Since 2012, he has been an Associate Professor of Mechanical and Electronic Engineering College, Shandong University of Science and Technology, China. His research interest includes material forming.